Available online at www.sciencedirect.com

SciVerse ScienceDirect

Ceramics International 38 (2012) 6865–6871

CERAMICS INTERNATIONAL

www.elsevier.com/locate/ceramint

Development of a surface roughness model in end milling of nHAP using PCD insert

Yaowei Yong[a,b], Sanket S. Kulkarni[b], Malgorzata Rys[b], Shuting Lei[b,*]

[a]School of Mechanical Engineering, Ningixa University, 750021 Yinchuan, Ningxia, PR China
[b]Industrial and Manufacturing Systems Engineering, Kansas State University, Manhattan, KS 66505, USA

Received 9 May 2012; accepted 26 May 2012
Available online 1 June 2012

Abstract

Similar physical properties with human bone make hydroxyapatite (HAP) a suitable bioceramic material for hard tissue replacement in the fields of orthopedics and dentistry. Before being used in the human body, HAP needs to be machined to the required shape and dimensions with minimal surface roughness. This study investigates the machinability of fully dense nano-crystalline hydroxyapatite (nHAP) bioceramic in milling operations using polycrystalline diamond insert (PCD). The focus is on the effects of various machining conditions on surface roughness. The first order and second order surface roughness models for the end milling of nHAP is developed using response surface methodology (RSM), relating surface roughness to the cutting parameters: cutting speed, feed, and depth of cut. Based on the experimental results, it is found that cutting parameters have significant effect on surface roughness. For the ranges used in this study, a low feed (0.002 mm/rev) results in a smooth surface, and the middle depth of cut (0.5 mm) should be avoided. The final results show that the combination of cutting speed $v=92$ m/min, feed $f=0.002$ mm/rev, and depth of cut $a_p=1.6$ mm gives a minimum surface roughness of 0.64 μm. In addition, it is proven that milling of nHAP is feasible for the fabrication of implants.

Keywords: (nHAP) nano-crystalline hydroxyapatite; Response surface methodology (RSM); Milling operation; Polycrystalline diamond insert

1. Introduction

Hydroxyapatite (HAP), whose chemical formula is written as $Ca_{10}(PO_4)_6(OH)_2$, is a bio-ceramic used as an artificial bone material substitute due to its good durability, esthetic values and good biocompatibility with human tissues [1]. It is a dense, non-porous surface reactive ceramic, which attaches directly to the bone by chemical bonding. Another reason for using it as a substitute in bone grafts is that the chemical and mechanical properties of HAP are very similar to those of bone and teeth [2]. HAP is bioactive, i.e. it supports bone ingrowth without breaking down, and it is stable in aqueous media with pH range of 4.2–8.0, which lowers the risk of implant corrosion [3]. As a calcium composite, HAP is considered as a brittle polycrystalline material, whose mechanical properties depend on material porosity, particle size [4], crystallinity, grain size, grain boundaries, and composition [5]. Generally speaking, high mechanical properties are accompanied by excellent crystallinity, lower porosity and fine grain [6]. For example, both strength and fracture toughness decrease dramatically with increasing porosity in porous HAP ceramics [7].

HAP can be employed in many forms such as powders, coating, porous blocks or fillers. HAP has been used in medicine and dentistry since it is similar to the natural bone though devoid of such organic constituents as collagen and polysaccharide [2–8]. It also behaves as a coating material on other bioinert metallic implant materials so as to enhance the adhesion between host and the substitute [9,10]. Recently, it was claimed that nano-crystalline HAP (nHAP) offers more advantages than conventional HAP materials. nHAP can improve fracture toughness and other critical mechanical properties. It was suggested that nHAP may be an ideal biomaterial due to its good biocompatibility and bone integration ability [11].

In spite of these superior biological properties, the high brittleness of nHAP makes it very difficult to shape after

*Corresponding author. Tel.: +1 785 532 3731.
E-mail address: lei@ksu.edu (S. Lei).

0272-8842/$36.00
http://dx.doi.org/10.1016/j.ceramint.2012.05.087

sintering without compromising surface quality. Generally, the most widely used finishing operation for ceramic materials is grinding, but it is time consuming because of its low material-removal rate and often causes surface/subsurface damage. In recent years, injection molding has been used for the fabrication of those biomaterials. However, the mold and the accessories used in injection molding are very costly, especially for highly specialized and customized implant products such as jaw bone implants [12].

Machining processes such as turning and milling may be used for bioceramics. In machining, surface integrity is one of the most important requirements, and its major indicator is surface roughness. Surface roughness depends on the tool geometry such as nose radius, rake angle, and cutting conditions such as cutting speed, feed and depth of cut [13]. Chelule et al. [14] studied the machinability of CAPTAL'90 HAP and found that chip fragments have sizes and shapes that are exact fit of the surface topography. The material has poor machinability and the surface roughness is insensitive to cutting conditions, perhaps due to porous nature of the material.

From the above literature review, it is found that the milling operation of nHAP is a promising method in the fabrication of bio-ceramics with low cost and high efficiency. This study aims to understand the characteristics of machinability of nHAP in milling, with a focus on surface roughness, and attempts to optimize the machining parameters to minimize the surface roughness.

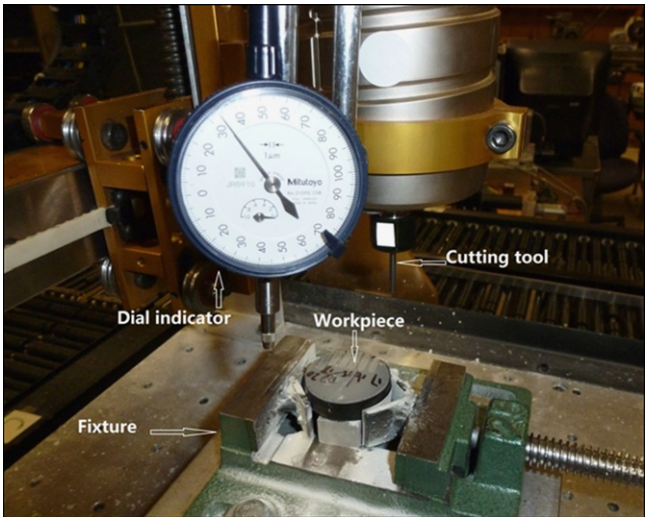

Fig. 1. Setup of the milling experiments.

2. Experimental procedure

2.1. Experimental setup

The experimental setup for the milling operation is shown in Fig. 1. All the machining experiments are conducted on a precision CNC milling machine, which has a maximum spindle speed of 22,000 rpm and minimum displacement of 5 μm. The nHAP samples used are round and polished, and the dimensions are approximately 40 mm in diameter and 15 mm in thickness. The workpiece is fixed by a V-shaped fixture, which can provide an even distribution of pressure around the sample and hold the workpiece in stable condition. For each experiment, the flatness of the workpiece surface is tested by a dial indicator so that the depth of cut is uniform during milling.

The surface roughness of the machined workpiece is measured using a Mitutoyo SJ-4000 profilometer. At the end of the experiments, the collected chip fragments and cutters are examined using an optical microscope. A one-flute polycrystalline diamond end mill with the diameter of 3.175 mm is used in the experiments.

The specimens of nano-crystalline hydroxyapatite in this study were developed and provided by Pioneer Surgical Technology, the detailed mechanical properties are shown in Table 1.

2.2. Design of experiments

The design of experiments (DOE) has a significant effect on the number of experimental runs; at the same time, it is a powerful analysis tool for modeling and analyzing the control factor's influence on response. Therefore, it is necessary to implement a qualified DOE, which is the convenient way to model a complex system with only a small set of experimental runs. However, a small set of factors can only build a simple model, but a large number of factors will cause too many runs of experiment. Thus, the necessities of selecting a suitable DOE seem to be very important. In the present research the response surface methodology (RSM) is utilized to arrange experimental runs and predict the surface roughness under the milling

Table 1
nHAP properties.

Compressive strength (MPa)	Bending strength (MPa)	Fracture toughness (MPa.m$^{1/2}$)
879 ± 56	330 ± 18	1.3 ± 0.2
3-Pt bending strength (MPa)[a]	Compressive strength (MPa)[a]	Tensile strength (MPa)[b]
330–356	877 ± 42	112–179

[a](3 mm dia × 20 mm).
[b](5 mm dia × 12.5 mm).

conditions. A five level, three variable central composite design (CCD) is applied to determine the best combination of cutting variables for the surface roughness. The range and center point values of three independent variables are based on the results of the previous experiments which also studied the same material in turning [15] and milling [16]. Totally 20 runs are carried out with 8 corner points, 6 axis points and 6 central points. Fig. 2 shows this central composite design. There are five levels for each factor, the value of α, 1.68, is determined by software (Minitab), and the values of the factors are chosen and coded based on a logarithm, as shown in Eq. (1) [17,18]:

$$c_i = \frac{\ln x_i - \ln x_{icenter}}{\ln x_{iHigher} - \ln x_{icenter}} \quad (i = v, f, a_p) \tag{1}$$

Where c_i is the coded value for a cutting parameter corresponding to its value x_i, $x_{icenter}$ is the value of every cutting parameter corresponding to the center (0), and $x_{iHigher}$ is the value of every cutting parameter corresponding to the higher level (+1). The machining variables are listed in Table 2.

The surface roughness model for the milling process in terms of the cutting parameters can be expressed as

$$R_a = C v^{\alpha} f^{\beta} a_p^{\gamma} \tag{2}$$

where v is the cutting speed, f is the feed, a_p represents the depth of cut, and R_a is the estimated surface roughness. In order to transfer the equation to the linear equation, the logarithmic transformation can be used, and then the equation can be formulated as follows:

$$\ln R_a = \ln C + \alpha \ln v + \beta \ln f + \gamma \ln a_p \tag{3}$$

To determine the behavior of this system, the above equation can be explained by the following equation:

$$y = b_0 + b_1 x_1 + b_2 x_2 + b_3 x_3 \tag{4}$$

where y represents the surface roughness on a logarithmic scale, x_i (i=1,2,3) represent the cutting speed, feed rate and depth of cut respectively, while the coefficient b_i (i=0,1,2,3) are the parameters to be estimated.

The 2nd order model can be written as

$$\widehat{Y} = b_0 + \sum_{i=1}^{3} b_i x_i + \sum_{i=1}^{3} b_{ii} x_i^2 + \sum_{i<j}^{3} b_{ij} x_i x_j \tag{5}$$

where: $\widehat{Y}$ is the estimated response based on the 2nd order model,

b_0 is an intercept, b_i b_{ii} and b_{ij} are the coefficients of the linear, quadratic and interactive terms, respectively.

And accordingly x_i and x_j represent the coded independent variables. The surface and contour plots are expressed according to the fitted equation so as to visualize the relationship between the experimental parameters and response and to achieve the optimum conditions [19].

According to the analysis of variance (ANOVA), the regression coefficients of the linear, quadratic and interaction terms are calculated. The regression coefficients were then used to make statistical calculations to generate dimensional and contour plots from the regression models. The Minitab (Version 16, USA) software package is used to analyze the experimental data.

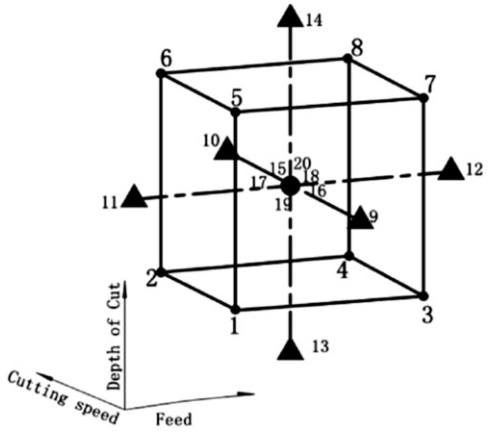

Fig. 2. Representation of central composite design.

3. Results and discussion

3.1. Surface roughness

The average surface roughness R_a of the machined surface is measured using a Mitutoyo SJ-4000 profilometer. R_a, also known as arithmetical mean roughness, is rated as the arithmetic average deviation of the surface valleys and peaks expressed in micrometers. The randomized cutting experiments of total 20 runs are measured. Every run is measured four times in different places along the cut, and the center point surface roughness is the average of the six average values of the center point runs. Table 3 shows the measurement results.

Table 2
Levels of variables and coding identification.

Factors (cutting parameters)	Levels				
	Lowest (−1.68)	Lower (−1)	Center (0)	Higher (+1)	Highest (1.68)
Cutting speed (v, m/min)	92	104	125	150	170
Feed rate (f, mm/rev)	0.002	0.0025	0.005	0.01	0.016
Depth of cut (a_p, mm)	0.16	0.25	0.5	1	1.6

From the experimental results, empirical equations can be developed to predict the surface roughness and to determine the significant parameters. Generally, the linear model can simplify the process and make the model easily understand, and the second order model is developed to describe the relationship between the inputs (investigated parameters) and the response (surface roughness) more accurately. In this research, ANOVA analysis of the Minitab software package was used to study the effect of machining parameters.

3.2. Development of the linear model

The first order surface roughness model based on the experiments is

$$y = 2.122 - 0.11466x_1 + 0.305173x_2 - 0.168946x_3 \quad (6)$$

The transformed equation of surface roughness value as a function of cutting speed (v), feed (f), and depth of cut (d) is as follows:

$$R_a = 1808.04 v^{-0.63} f^{0.44} a_p^{0.24} \quad (7)$$

Eq. (7) is derived from Eq. (6) by substituting the coded values of x_1, x_2 and x_3 in terms of $\ln v$, $\ln f$ and $\ln a_p$.The ANOVA of the linear model is listed in Table 4.

The Model F-value of 5.03 implies that the model is significant. There is only a 2% chance that a ''Model F-Value'' this large could occur due to noise. For the three cutting parameters, only feed has a significant influence on surface roughness (p-value < 0.05) under the chosen conditions. But the predicted R^2 value is small (58%) which demands a higher order model with square and quadratic terms if it will be used for accurate prediction.

From the equation, it is found that an increase in cutting speed (x_1) and depth of cut (x_3) results in a decrease in surface roughness value (y),, and an increase in feed will give an increase in surface roughness.

3.3. Development of the second order model

Because the linear model has a significant lack of fit, the quadratic model is developed to predict the results. The second order surface roughness model in the coded form is built based on the experimental results as described below, and the ANOVA is shown in Table 5:

$$\widehat{Y} = 2.26845 + 0.305173x_2 - 0.168945x_3 + 0.19125x_2x_3 - 0.230286x_3^2 \quad (8)$$

From the ANOVA table, the model regression value of F is 8.16, which means that the model is significant.

Table 3
Results of surface roughness and cutting conditions.

Cutting speed (rev/min)	Feed (mm/rev)	Depth of cut (mm)	Surface roughness (μm)
12,532	63	0.5	23
12,532	63	1.6	1.3
10,443	104	1	2.72
9222	46	0.5	2.5
17,029	85	0.5	2.11
12,532	201	0.5	2.87
10,443	104	0.25	2.53
10,443	26	1	1.22
15,038	150	1	2.23
12,532	25	0.5	1.92
15,038	38	1	1.68
12,532	63	0.16	2
15,038	38	0.25	1.75
15,038	150	0.25	2.22
10,443	26	0.25	2.4

Table 4
ANOVA of the first order RSM model.

Source	DF	Seq SS	Adj SS	Adj MS	F	P
Regression	3	1.84122	1.84122	0.61374	5.03	0.02
linear	3	1.84122	1.84122	0.61374	5.03	0.02
A	1	0.17955	0.17955	0.17955	1.47	0.25
B	1	1.27187	1.27187	1.27187	10.43	0.008
C	1	0.3898	0.3898	0.3898	3.2	0.101
Residual error	11	1.34122	1.34122	0.12193		
Total	14	3.18244				

In this research it is very clearly seen that the feed and depth of cut influence the surface roughness. It also can be seen that the nonlinear terms have effect on the surface roughness, but only the depth of cut quadratic term and the interaction of feed and depth of cut affect the surface roughness significantly, while others do not have a significant influence on surface roughness.

The fitted model is used to analyze the effects of cutting parameters on the surface roughness values and to optimize the cutting conditions in the given ranges. It is possible to select the combination of cutting speed, feed, and depth of cut which would reduce surface roughness, while achieving a desired machining efficiency. Figs. 3,and 5 are the contour plots of the surface roughness (R_a) at the high level (1 mm) of depth of cut.Fig. 4

The plots suggest that the feed should be lower with an appropriate cutting speed while the depth of cut should avoid the middle levels. During the experiments, the chips of nHAP are in a form of powders except for some relatively large crack-chips on the top of workpiece surface. By observing the crack-chips, it is found that the shape and dimensions of all crack-chips are similar, like a half-moon in shape. Those crack-chips are formed when the feed is at the high level and the depth of cut at the low level. Because the chosen tool is a single flute cutter, it will cause intermittent force and vibration on the workpiece. An increase in feed means an increase in chip load; and the larger the chip load is, the larger the cutting force will be. Since the fracture toughness of nHAP is very low, once the cutting force is up to the fracture strength, it may cause the irregular fracture chips from the surface, therefore the rough surface is formed.

From the results, it is found that either increasing or decreasing the depth of cut from the middle value results in a better surface roughness. Generally, a large depth of cut should be chosen in practice to improve the productivity of operations.

During the experiments, tool wear is always being inspected. The results show that there is a very little tool wear in the PCD insert, about 0.05 mm in 20 runs (see Fig. 6). The PCD insert is very wear resistant as compared with the

Table 5
ANOVA of the second order RSM model.

Source	DF	Seq SS	Adj SS	Adj MS	F	P
Regression	9	2.9796	2.9796	0.33107	8.16	0.016
Linear	3	1.84122	1.84122	0.61374	15.13	0.006
Speed	1	0.17955	0.17955	0.17955	4.43	0.089
Feed	1	1.27187	1.27187	1.27187	31.35	0.003
Depth	1	0.3898	0.3898	0.3898	9.61	0.027
Square	3	0.69594	0.69594	0.23198	5.72	0.045
Speed × Speed	1	0.06836	0.00001	0.00001	0	0.988
Feed × Feed	1	0.30659	0.00664	0.00664	0.16	0.703
Depth × Depth	1	0.32099	0.32099	0.32099	7.91	0.037
Interaction	3	0.44244	0.44244	0.14748	3.64	0.099
Speed × Feed	1	0.05951	0.05951	0.05951	1.47	0.28
Speed × Depth	1	0.09031	0.09031	0.09031	2.23	0.196
Feed × Depth	1	0.29261	0.29261	0.29261	7.21	0.044
Residual Error	5	0.20284	0.20284	0.04057		
Total	14	3.18244				

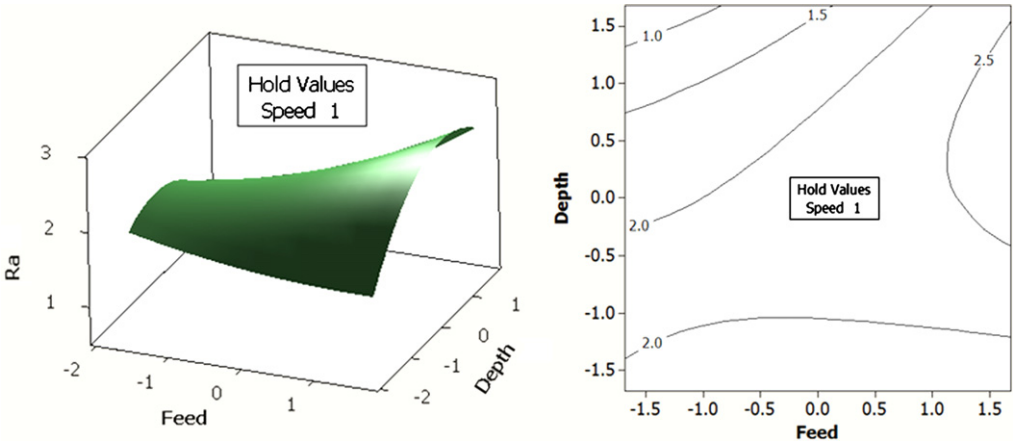

Fig. 3. Surface and contour plot of surface roughness vs. feed and depth of cut.

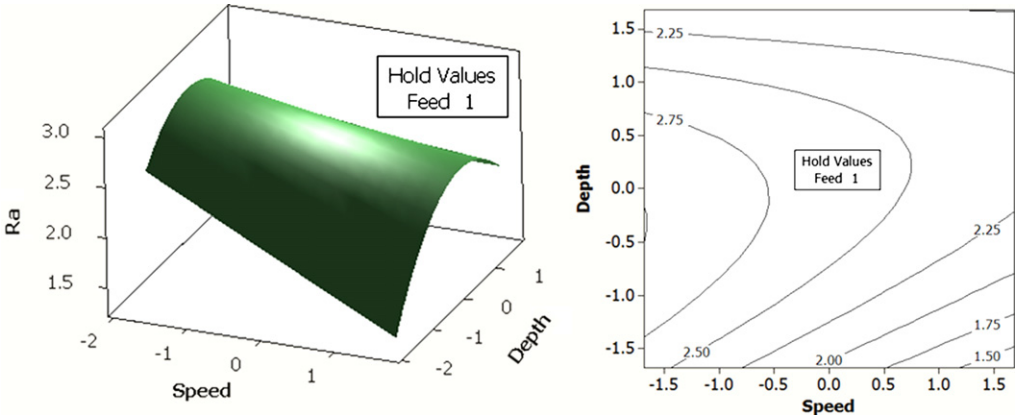

Fig. 4. Surface and contour plot of surface roughness vs. cutting speed and depth of cut.

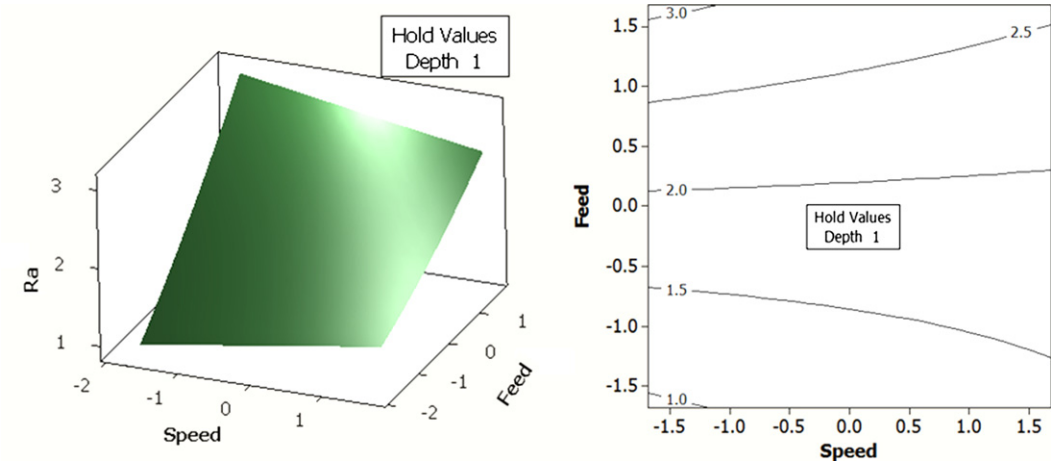

Fig. 5. Surface and contour plot of surface roughness vs. cutting speed and feed.

carbide tool in milling the nHAP materials. The carbide insert develops a large tool wear just after the first run as observed by Kulkarni et al. [16]. Therefore, PCD may be a more suitable cutting tool for nHAP.

3.4. Optimization of surface roughness

Optimizations of the operating parameters not only increase the machining economics and machining efficiency, but also improve the product quality to some extent. In this research an effort has been made to build the prediction model to produce the best possible surface roughness within the parameters' range.

The problem of optimization of surface roughness can be stated as follows: minimize surface roughness (R_a) using the model given here:

$$\widehat{Y} = 2.26845 + 0.305173x_2 - 0.168945x_3 + 0.19125x_2x_3 - 0.230286x_3^2 \quad (9)$$

Subjected to:

Cutting speed: $92\ m\ /\ \min \le v \le 170\ m\ /\ \min$

Feed: $0.002\ mm\ /\ rev \le f \le 0.016\ mm\ /\ rev$

Depth of cut: $0.16\ mm \le a_p \le 1.6\ mm$

where x_1, x_2 and x_3 are the logarithmic transformation of cutting speed, feed and depth of cut, respectively. To optimize the surface roughness, Minitab is used to predict the best combination of these parameters. The final results show that the combination of $x_1 = -1.68 (v = 92\ m\ /\ \min)$, $x_2 = -1.68 (f = 0.002 mm\ /\ rev)$ and $x_3 = 1.68 (a_p = 1.6\ mm)$ gives a minimum surface roughness. Then the confirmation experiment is done and it is shown that the measured result is 0.64, which is the smallest value in all the experimental runs and confirmation runs.

4. Conclusions

1. Response surface methodology is a useful and powerful technique for surface roughness prediction. This method uses a small set of experiments to generate a great deal of information to develop the model equations for surface roughness.
2. According to the results and analysis, it is found that the input parameters such as feed and depth of cut are the significant factors on the surface roughness. Also, the interaction of depth and feed and the quadratic term

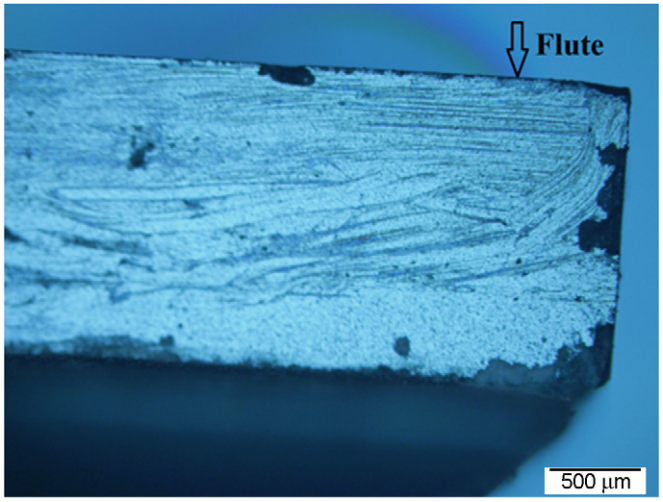

Fig. 6. Tool wear after 20 runs.

of depth of cut are the significant factors.

3. The first order model is found to be inadequate based on the statistical analysis, and the second order model is developed to predict the surface roughness more accurately.
4. The results show that the surface roughness increases with feed. The depth of cut should be avoided in the middle level (0.5 mm) to obtain a fine surface. Also, a high depth of cut can be chosen in order to improve the machining efficiency.
5. Milling operation is proven to be feasible for the nHAP bioceramic.

Acknowledgments

The authors would like to thank Pioneer Surgical Technology, Inc. for providing the nHAP samples used in this study.

References

[1] J.C. Le Huec, T. Schaeverbeke, D. Clement, J. Faber, A. Le Rebeller, Influence of porosity on the mechanical resistance of hydroxyapatite ceramics under compressive stress, Biomaterials 16 (2) (1995) 113–118.
[2] J. Park, Hydroxyapatite, in: Bioceramics—Properties, Characterizations, and Applications, Springer, New York, 2009, pp. 177–197.
[3] V.A. Dubok, BioceramicsYesterday, today, omorrow, Powder Metallurgy and Metal Ceramics 39 (7) (2000) 381–394.
[4] Y. Mostafa Nasser, Characterization, thermal stability and sintering of hydroxyapatite powders prepared by different routes, Materials Chemistry and Physics 94 (2–3) (2005) 333–341.
[5] F. Pecqueux, F. Tancret, N. Payraudeau, J.M. Bouler, Influence of microporosity and macroporosity on the mechanical properties of biphasic calcium phosphate bioceramics: modelling and experiment, Journal of the European Ceramic Society 30 (4) (2010) 819–829.
[6] S.V. Dorozhkin, Calcium orthophosphates as bioceramics: state of the art, Journal of Functional Biomaterials 1 (1) (2010) 22–107.
[7] W. Suchanek, Processing and properties of hydroxyapatite-based biomaterials for use as hard tissue replacement implants, Journal of Materials Research 13 (01) (1998) 94.
[8] A. Bauermeister, R. Maatz, A method of bone maceration; results in animal experiments., The Journal of Bone and Joint Surgery-American Volume 39 (1) (1957) 153.
[9] Joon Park, Roderic Lakes, Metallic Implant Materials —Biomaterials, Springer, New York, 2007 99–137.
[10] W.R. Moore, S.E. Graves, G.I. Bain, Synthetic bone graft substitutes, ANZ Journal of Surgery 71 (6) (2001) 354–361.
[11] H. Zhou, J. Lee, Nanoscale hydroxyapatite particles for bone tissue engineering, Acta Biomaterialia 7 (7) (2011) 2769–2781.
[12] C. Hengky, B. Kelsen, S. Saraswati, P. Cheang, Mechanical and biological characterization of pressureless sintered hydroxapatite–polyetheretherketone biocomposite, in: Proceedings of the 13th International Conference on Biomedical Engineering, Springer, Berlin Heidelberg, 2009, pp. 261–264.
[13] N. Galanis, D. Manolakos, Surface roughness prediction in turning of femoral head, International Journal of Advanced Manufacturing Technology 51 (1) (2010) 79–86.
[14] K.L. Chelule, T. Coole, D.G. Cheshire, An investigation into the machinability of hydroxyapatite for bone restoration implants, Journal of Material Processing Technology 135 (2–3) (2003) 242–246.
[15] S.S. Kulkarni, M. Haynes, L. Reimers, K.R. Achanta, S. Lei, An investigation into machinability of sintered nanocrystalline hydroxyapatite, ASME Conference Proceedings 44304 (2011) 73–79.
[16] S.S. Kulkarni, Y. Yong, M. Rys, S. Lei, Machining assessment of nano-crystalline hydroxyapatite bio-ceramic, in:Proceedings of the 40th North American Manufacturing Research Conference (NAMRI/SME) ,vol. 40, 2012, p. 8.
[17] A. Mansour., H. Abdalla, Surface roughness model for end milling: a semi-free cutting carbon casehardening steel (EN32) in dry condition, Journal of Materials Processing Technology 124 (1–2) (2002) 183–191.
[18] K.C. Lo, N.N.S. Chen, Prediction of tool life in hot machining of alloy-steels, International Journal of Production Research 15 (1) (1977) 47–63.
[19] X. Yin, Q. You, Z. Jiang, Optimization of enzyme assisted extraction of polysaccharides from Tricholoma matsutake by response surface methodology, Carbohydrate Polymers 86 (3) (2011) 1358–1364.